Altered morpho-functional features of bones in autoimmune disease-prone BXSB/MpJ-*Yaa* mice

Short title: Bone pathology in autoimmune disease-prone mice

Takashi Namba[1], Osamu Ichii[1]*, Teppei Nakamura[1,2], Md. Abdul Masum[1], Yuki Otani[1], Saori Otsuka-Kanazawa[1], Yaser Hosny Ali Elewa[1,3], and Yasuhiro Kon[1]

[1]Laboratory of Anatomy, Department of Basic Veterinary Sciences, Faculty of Veterinary Medicine, Hokkaido University, 060-0818, Japan; [2]Section of Biological Safety Research, Chitose Laboratory, Japan Food Research Laboratories, 066-0052, Japan; [3]Department of Histology and Cytology, Faculty of Veterinary Medicine, Zagazig University, 44519, Egypt

Corresponding author: Osamu Ichii, D.V.M., Ph.D.

Laboratory of Anatomy, Department of Basic Veterinary Sciences, Faculty of Veterinary Medicine, Hokkaido University, Kita 18-Nishi 9, Kita-ku, Sapporo, JAPAN.

Tel & Fax: +81-11-706-5189, Email: ichi-o@vetmed.hokudai.ac.jp

Abstract

Bones play crucial roles in motility, electrolyte metabolism, and immunity. Clinical cases have suggested bone dysfunction in several systemic autoimmune diseases. This study exhibited altered bone morpho-functions in BXSB/MpJ-*Yaa* as a murine autoimmune disease model. During clinical examinations, the serum Ca level was significantly higher in BXSB/MpJ-*Yaa* than the healthy control BXSB/MpJ at the early stage (2-4 months), but that in BXSB/MpJ-*Yaa* decreased with advancing age. Further, the increase of urinary Ca with nephritis and white blood cells with mild anemia proceeded in BXSB/MpJ-*Yaa* with advancing age. The thyroid and parathyroid gland morphologies and serum parathormone level did not differ among strains, but the tibia was smaller in BXSB/MpJ-*Yaa* than in BXSB/MpJ especially during the late stage (6 months). Histologically, osteoclasts and osteoblasts showed increased and decreased tendencies, respectively, in BXSB/MpJ-*Yaa* during the early stage, and osteoclasts and bone area significantly increased and decreased, respectively, compared with BXSB/MpJ at later stages. The bone morphological indices were affected by the expression of BXSB/MpJ-*Yaa* mutation genes and inflammatory genes in BXSB/MpJ-*Yaa*. In conclusion, systemic autoimmune diseases in BXSB/MpJ-*Yaa* are associated with the morpho-functional abnormalities of bones, calcium dynamics, and hematopoiesis, and each factor contributes to forming the phenotypes in this disease.

Keywords: autoimmune disease, BXSB/MpJ-*Yaa*, bone, calcium, hematology, histopathology

Impact statement

Bone disease, such as osteoporosis and rheumatoid arthritis, increases because of the progression of an aging society. Autoimmune disease are important and predisposing factors for the pathogenesis of the bone disease, however, the pathological mechanism is unclear. We have demonstrated that systemic autoimmune disease in BXSB/MpJ-*Yaa* is closely associated with the morpho-functional abnormalities of bones including bone marrow and has complicated pathology. The abnormalities are characterized by altered regulations of serum calcium, anemia tendency, and hematopoiesis with increased WBCs and decreased PLs, short length and low mass of long bones, imbalance in the populations of osteoclasts and osteoblasts, and increased expression of candidate genes for causing and/or exacerbating their phenotypes. Therefore, BXSB/MpJ-*Yaa* serves as a model to elucidate bone phenotypes in systemic autoimmune disease that would be affected by the factors in the bone as well as the other immune and/or mineral metabolism organs both in human and experimental medicine.

Introduction

Bones play various roles, such as assisting motor function and electrolyte metabolism of circulating calcium or phosphorus. Additionally, the bone marrow (BM), a primary lymphatic organ located deep in the bone, plays a crucial role in immunity. To date, the bone and BM have been considered different and unrelated organs owing to the differences in their development and functions. However, recently, the osteoblasts responsible for bone formation were shown to participate in the production of hematopoietic stem and progenitor cells (HSPCs) in mice.[1] Moreover, osteoclast precursor cells and osteoblasts expressed tumor necrosis factor receptor superfamily, member 11a, nuclear factor kappa B (NFκB) activator (Tnfrsf11a/RANK), and tumor necrosis factor (ligand) superfamily, member 11 (Tnfsf11/RANKL), respectively.[2] This cell to cell contact via RANK/RANKL interaction was important for the differentiation of mouse osteoclast precursor cells into mature osteoclasts.[2] Alternatively, RANKL expression was identified in T-cells. It regulates interactions between T-cells and dendritic cells, maturing dendritic cells, and lymph node organogenesis in humans.[3,4]

The functional imbalance of osteoblasts and osteoclasts causes bone-related diseases such as osteoporosis in humans, and their incidents increase because of the progression of an aging society.[5,6] Osteoporosis and osteopetrosis are associated with the hyper-activation and dysfunction of osteoclasts causing the decrease and increase in bone density, respectively.[6,7]

Particularly, aging and altered immune conditions are important and predisposing factors for the pathogenesis of osteoporosis. Rheumatoid arthritis (RA), a bone-related autoimmune disease in humans, causes chronic inflammation characterized by secondary osteoporosis and synovitis, joint swelling, and destruction of cartilage and bone.[8,9] RA patients develop motor impairment with arthralgia, and bone destruction that could be induced by the actions of T helper 1 (Th1)-cells, Th17-cells, B-cells, and produced cytokines, such as tumor necrosis factor α (TNF-α), interleukin 1 (IL-1), and IL-6.[8,10–13] Thus, crucial correlations between the bone and immune system based on osteoimmunology, and their alternations would contribute to their bidirectional pathogenesis.

For the diagnosis and evaluation of bone-related diseases, blood electrolyte examination, targeting Ca and phosphorus, is useful. However, their blood concentration does not completely reflect bone conditions. Blood Ca concentration is regulated by various organs such as bones, thyroid glands, parathyroid glands, kidneys, and intestines with regard to absorption and excretion.[14,15] During the dysfunction of Ca-regulating organs, its blood concentration would be changed. Although the chronic kidney disease (CKD) patients exhibited hypocalcemia and hyperphosphatemia due to impaired renal functions, these imbalances are compensated by an increased activity of parathyroid hormone (PTH). However, with the progression of CKD, PTH cannot control the blood Ca, which shows significant decrease.[16] Further, vitamin D obtained through food, produced in the skin, and

activated in the kidney, is related to osteogenesis by increasing blood Ca level.[14] Vitamin D also associates with the immune function and its abnormality. Patients with autoimmune diseases, such as systemic lupus erythematosus (SLE) and RA, have low levels of vitamin D in the blood, contributing to osteoporosis.[17] Furthermore, the blood mineral levels show complex dynamics and do not necessarily represent the state of bones in several diseases. Therefore, the combination of morphological evaluations of bones and blood examinations is essential to understand the pathogenesis of bone-related diseases in the patients suffering the other disease.

To understand the effect of autoimmune diseases on bone morphology, we histopathologically examined the phenotype of BXSB/MpJ-*Yaa* (BXSB-Yaa) mice as an autoimmune disease model. As BXSB-Yaa carries the Y-linked autoimmune accelerator (*Yaa*) mutation on the Y chromosome, the male mice develop severe autoimmune symptoms similar to SLE characterized by abnormal proliferation of B-cells, auto-antibody production, and splenomegaly,[18,19] but not RA.[20] We have already demonstrated the pathological features of nephritis and dacryoadenitis in BXSB-Yaa,[21–23] however, its bone morphology was unclear. Therefore, we analyzed the altered bone structures, especially focusing on the population of osteoblasts and osteoclasts, by comparisons between BXSB-Yaa and its control strain BXSB/MpJ (BXSB) with the evaluation of blood mineral dynamics and autoimmune disease conditions.

Material and methods

Animal ethics

Animal experimentation was approved by the Institutional Animal Care and Use Committee of the Graduate of School of Veterinary Medicine, Hokkaido University (approval No.16-0124). The animals were handled in accordance with the Guide for the Care and Use of Laboratory Animals, Graduate School of Veterinary Medicine, Hokkaido University (approved by the Association for Assessment and Accreditation of Laboratory Animal Care International). Male BXSB and BXSB-Yaa aged 2-6 months were purchased from Japan SLC, Inc. (Hamamatsu, Japan) and were maintained under specific pathogen-free conditions. Blood of all mice were collected from femoral arteries under deep anesthesia using the mixture of medetomidine (0.3 mg/kg), midazolam (4 mg/kg), and butorphanol (5 mg/kg). Finally, all mice were euthanized by cervical dislocation.

Hematological and serological analysis and urinalysis

The number of white blood cells (WBCs), red blood cells (RBCs), platelets (PLs), hemoglobin concentration (HC), hematocrit volume (Ht), mean corpuscular volume (MCV), and mean corpuscular HC (MCHC) was measured using a XT-1800i instrument (Sysmex Corporation; Kobe, Japan). Additionally, the blood smear was stained by Diff-Quik solution (Sysmex Corporation) to detect reticulocytes.

Serum levels of anti-double strand DNA (dsDNA) antibody were measured to evaluate systemic autoimmune conditions using LBIS Anti dsDNA-Mouse ELISA Kit (FUJIFILM Wako Pure Chemical Corporation; Osaka, Japan) according to the manufacturer's instructions. As an index of mineral metabolism of bones, the serum Ca concentration was measured using a Fuji Dri-Chem 7000v instrument (FUJIFILM Medical Co., Ltd.; Tokyo, Japan). Furthermore, urinary concentrations of Ca and creatinine (CRE) were determined by a Fuji Dri-Chem 7000v instrument (FUJIFILM Medical Co., Ltd.) and Creatinine-test-Wako (FUJIFILM Wako Pure Chemical Corporation) according to the manufacturer's instructions. Serum PTH concentration was measured to evaluate parathyroid gland function using Mouse PTH 1-84 ELISA kit (Quidel Corporation; San Diego, CA, USA).

Morphological and histological analyses of bones

To evaluate the gross morphology of bones, the bone length and wet weight were measured. After taking a picture of the tibia, the tibia length was measured by ImageJ.[24] Subsequently, the ratio of tibia and fibula weight to body weight (BW) was calculated.

The tibia samples for histology were fixed with 4% paraformaldehyde at 4°C overnight, and decalcified by 5% ethylenediaminetetraacetic acid at 4°C for 5 days. After decalcification, the specimens were routinely dehydrated by ethanol and embedded into paraffin. Then, paraffin sections (3 μm) were prepared and stained with hematoxylin and eosin (HE) or

147 tartrate-resistant acid phosphatase (TRAP) staining Kit (FUJIFILM Wako Pure Chemical
148 Corporation) to detect the osteoclasts.
149
150 ***Immunohistochemistry***
151 The paraffin sections were immunostained using the methodology by a previous study.[23] The
152 antigen retrieval was applied to sections (Supplementary Table 1). Subsequently, to block
153 internal peroxidase activity, the sections were soaked in methanol containing 0.3% H_2O_2 for
154 20 minutes at 25°C. After washing three times in phosphate-buffered saline (PBS), the
155 sections were incubated with a blocking serum for 1 h at 25°C to block the non-specific sites.
156 Then, sections were incubated with primary antibodies overnight at 4°C. The sections were
157 then washed thrice in PBS and incubated with secondary antibodies for 30 minutes at 25°C
158 and washed thrice in PBS. Consequently, the sections were incubated with streptavidin
159 conjugated horseradish peroxidase (SABPO(R) kit, Nichirei; Tokyo, Japan) for 30 minutes at
160 25°C, washed three times in PBS, and the immunopositive reaction was visualized with
161 3,3'-diaminobenzidine tetrahydrochloride-H_2O_2 solution. Finally, the sections were lightly
162 stained with hematoxylin. The details of the antibody, antigen retrieval, and blocking are
163 listed in Supplementary Table 1.
164
165 ***Histoplanimetry***

166 We performed the histoplanimetrical analysis of tibias using histological stained sections as
167 shown in Supplementary Fig. 1. We evaluated the area ratio of bone to BM, the ratio of
168 trabecular area to tissue area (Tb.Ar/T.Ar), trabecular width (Tb.Wi), trabecular number
169 (Tb.N), trabecular separation (Tb.Sp), $TRAP^+$ cells with 2 or more nuclei, as osteoclasts,
170 $osteocalcin^+$ cells, osteoblasts, and osteocytes. [25,26]
171
172 ***Quantitative polymerase chain reaction (qPCR)***
173 Total RNA from the bone including BM in a humerus was purified using the TRIzol reagent
174 (Thermo Fisher Scientific; Waltham, MA, USA) following the manufacturer's instructions.
175 The purified total RNA (83.3 ng/μl) was treated as a template to synthesize cDNA using
176 ReverTra Ace qPCR RT Master Mix (TOYOBO CO., LTD.; Osaka, Japan). Quantitative PCR
177 analysis was performed on the cDNA (20 ng/μl) using THUNDERBIRD® SYBR® qPCR
178 Mix (TOYOBO CO., LTD.) and the following gene-specific primers (Supplementary Table 2).
179 The qPCR cycling conditions were: 95°C for 1 min, (95°C for 15 s, 60°C for 45 s [40 cycles]).
180 Data were normalized by the values of actin, beta (*Actb*), and those of BXSB at 3 months
181 using the delta-delta Ct method.
182
183 ***Statistical analysis***
184 The data were expressed as the mean ± standard error (SE) and statistically analyzed by a

non-parametric manner. Briefly, the significance between the two groups was analyzed by the Mann-Whitney *U*-test ($P < 0.05$). The correlation between the two parameters was analyzed using Spearman's correlation test ($P < 0.05$).

Results

Autoimmune disease features found in BXSB-Yaa

We pathologically examined mice at 3 and 6 months of age (Fig. 1). The BW in BXSB-Yaa was lower than in BXSB at both ages, and that of BXSB significantly increased with advancing age, but not in BXSB-Yaa (Fig. 1(a)). Regarding autoimmune disease indices, BXSB-Yaa showed significantly higher values in the ratio of spleen weight to BW (S/B) and the serum levels of anti-dsDNA antibody compared with BXSB at both ages (Fig. 1(b) and (c)). Further, for S/B, BXSB-Yaa at 6 months significantly showed higher values than those at 3 months (Fig. 1(b)). Thus, autoimmune disease phenotypes were evident in BXSB-Yaa and deteriorated at 6 months.

Impaired bone metabolism, renal function, and hematopoiesis in BXSB-Yaa

Considering bone metabolism indices, the serum level of Ca was significantly higher in BXSB-Yaa than in BXSB at 2-4 months, and that of the former was significantly decreased with advancing age (Fig. 1(d)), indicating the imbalanced Ca metabolism in BXSB-Yaa. For the ratio of urinary Ca to CRE level, an indicator of urinary Ca excretion, the BXSB-Yaa at 6 months showed the highest value, and significant differences were observed between 3 and 6 months in this strain (Fig. 1(e)). Although we hypothesized secondary hyperparathyroidism in BXSB-Yaa at 6 months due to nephritis,[14] neither significant age nor strain-related change

was observed in the serum PTH concentration (Fig. 1(f)).

Furthermore, we performed hematological and serological analyses, focusing on hematopoiesis including, counts of WBCs, RBCs, PLs (Fig. 1(g-i)), HC, Ht, MCV, and MCHC (Fig. 1(j-m)). BXSB-Yaa showed significant increase and decrease in WBCs and PLs at 6 months compared with 3 months, respectively (Fig. 1(g) and (i)). Further, BXSB-Yaa at 6 months showed significant increase and decrease in MCV and MCHC compared with BXSB at the same age, respectively (Fig. 1(l) and (m)). There was no significant age or strain-related change in the other parameters. Further, at 6 months, the reticulocytes were more abundant in BXSB-Yaa than in BXSB (Fig. 1(n)).

We also histologically examined the organs, such as kidneys, thyroid and parathyroid glands, involved in the regulation of blood Ca concentration (Fig. 2(a-c)). For renal histopathology, severe glomerulonephritis with immune cell infiltrations to the tubulointerstitium was observed in the kidney of BXSB-Yaa at 6 months as described previously,[21] but that was not clearly observed in BXSB at both ages and BXSB-Yaa at 3 months (Fig. 2(a)). The injured kidney in BXSB-Yaa at 6 months coincided with increase in urinary Ca level (as shown in Fig. 1(e)). In thyroid glands, histopathological changes such as dilation of follicle or inflammation were not observed in all examined mice (Fig. 2(b)). Further, the localization and the number of immune-positive parafollicular cells for calcitonin, which decreases blood Ca level by inhibiting bone resorption, did not remarkably differ. Parathyroid glands were similarly

observed among all examined mice, and were surrounded by the connective tissues in thyroid glands (Fig. 2(c)). Similar to thyroid glands, no histopathological change including inflammation was observed within the parathyroid glands in all mice. Further, the localization and the number of immune-positive principal cells for PTH, increasing bone resorption, did also not remarkably differ.

Altered bone morphology in BXSB-Yaa

Macroscopically, during observation periods, the tibia of BXSB-Yaa were smaller, and BM was whiter compared to BXSB at 6 months (Fig. 3(a)) as associating with the increased WBCs and anemic phenotypes of BXSB-Yaa (Fig. 1(g), (l) and (n)). The tibia length and the weight of tibia and fibula significantly increased in BXSB with advancing age, but an age-related significant increase in BXSB-Yaa was only observed in the tibia length (Fig. 3(b) and (c)). Importantly, BXSB-Yaa exhibited significantly shorter and lighter tibia compared to BXSB at 6 months (Fig. 3(b) and (c)). Further, the ratio of tibia and fibula weight to BW in BXSB-Yaa at 6 months was significantly lower than in the same strain at 3 months or BXSB at 6 months (Fig. 3(d)).

Regarding the histopathological analysis of the tibias, we observed entire bone sections and identified drastic morphological changes around the epiphysis in BXSB-Yaa. Briefly, although no remarkable strain difference was observed at 3 months, the reduction of trabeculas and

245 thinning of compact bone was observed in BXSB-Yaa at 6 months (Fig. 3(e)). In the area ratio
246 of bone to BM, an indicator of bone thickness, BXSB-Yaa showed significantly lower values
247 compared with BXSB at 6 months (Fig. 3(f)). Further, to evaluate trabecular bones, we
248 examined Tb.Ar/T.Ar, Tb.Wi, Tb.N, and Tb.Sp, according to a parallel plate model (Fig.
249 3(g-j)).[25,26] Regarding the values of Tb.Ar/T.Ar, Tb.Wi, and Tb.N, BXSB-Yaa at 6 months of
250 age showed significantly lower values compared with the same strain at 3 months or BXSB at
251 6 months of age, and Tb.Wi in BXSB-Yaa at 3 months was also significantly lower than
252 BXSB at the same age (Fig.3 (g-j)). Additionally, BXSB-Yaa at 6 months of age showed
253 significantly higher values in Tb.Sp compared with BXSB-Yaa at 3 months and BXSB at 6
254 months of age (Fig.3 (j)). However, no significant difference was observed in the density of
255 osteocytes between the strains at both examined ages (Fig. 3(k)).
256
257 ***Altered number of osteogenesis-associated cells in BXSB-Yaa***
258 To evaluate osteoclasts, we observed the cells positive for TRAP, the enzyme produced by
259 osteoclasts.[27] $TRAP^+$ osteoclasts were mainly localized to the surface of the medullary cavity,
260 and were more abundant near the epiphyseal cartilages in both strains at both ages (Fig. 4(a)).
261 However, the enzyme activity of TRAP seemed to be stronger in BXSB-Yaa at 6 months
262 compared with other mice. These findings were confirmed by histoplanimetry, displaying that
263 the number of $TRAP^+$ osteoclasts was higher in BXSB-Yaa than in BXSB at both ages, and

264 significant difference was observed at 6 months (Fig. 4(c)).

265 Subsequently, we also evaluated osteoblasts by immunohistochemistry targeting the

266 osteocalcin produced by osteoblasts, which is generally regarded as a marker of bone

267 formation.[28] Similar to TRAP$^+$ osteoclasts, the osteocalcin$^+$ cells lined the surface of the

268 medullary cavity (Fig. 4(b)). There were no age or strain-related differences in the numerical

269 values of osteoblasts. However, BXSB-Yaa tended to display lower values compared to

270 BXSB at 3 months of age, and subsequently tended to increase with advancing age, in the

271 osteocalcin$^+$ osteoblasts (Fig. 4(d)).

272

273 ***mRNA expression of Yaa locus genes and inflammatory cytokines in BXSB-Yaa***

274 In order to identify the factors associated with autoimmune disease and bone abnormalities,

275 the mRNA expression of the humerus including BM was examined by qPCR. Firstly, we

276 examined the genes on the *Yaa* locus (Fig. 5), since BXSB-Yaa had the duplicated 15 genes

277 on Y chromosome because of translocation of X chromosome.[19] The genes, such as Rab9,

278 member of the RAS oncogene family (*Rab9*), tymosin β 4 X chromosome (*Tmsb4x*),

279 phosphoribosyl pyrophosphate synthetase 2 (*Prps2*), toll-like receptor 7 (*Tlr7*), and *Tlr8*, were

280 higher in BXSB-Yaa compared with BXSB at 3 and 6 months of ages without age-related

281 changes. Thus, the expression of the genes seemed to be increased by the influence of *Yaa*

282 mutation. Further, BXSB-Yaa significantly showed higher expression in MSL complex

subunit 3 (*Msl3*) and Rho GTPase activating protein 6 (*Arhgap6*) compared with BXSB at 6 months and BXSB-Yaa at 3 months. An age-related significant increase was observed in the expression of amelogenin X-linked (*Amelx*) in BXSB-Yaa, and this strain at 6 months also significantly showed higher expression in Midline 1 (*Mid1*) than BXSB at the same age. Consequently, the mRNA levels of inflammatory cytokines associating with bone resorption, such as *Il1a*, *Il1b*, *Il6*, *Il8*, and *Tnf*, were measured (Fig. 5).[10–12,29] The expression of *Il1a* and *Tnf* in BXSB-Yaa at 6 months was significantly higher than in BXSB at 6 months and in BXSB-Yaa at 3 months. Furthermore, the mRNA levels of *Il1b* in both strains at 6 months were higher than that at 3 months, and the increase of BXSB-Yaa was more significant.

Correlation between altered bone morphology and autoimmune disease in BXSB-Yaa

Correlation between the indices of bone morphology and autoimmune disease is shown in Table 1. The ratio of tibia and fibula weight to BW in all mice showed significant and negative correlations with S/B and mRNA expression of *Tlr8* and *Tlr7* in bones; and that in BXSB-Yaa showed significant and negative correlations with *Arhgap6* expression in bones. The area ratio of bone to BM showed significant and negative correlations with serum anti-dsDNA antibody levels and mRNA expression of *Rab9, Tmsb4x, Prps2, Msl3, Arphgap6,* and *Mid1* in bones; and that in BXSB-Yaa showed significant and negative correlations with *Tmsb4x, Prps2,* and *Msl3* expression in bones. Tb.Ar/T.Ar showed significant and negative

correlations with S/B, serum anti-dsDNA antibody levels, and mRNA expression of *Tmsb4x*, *Tlr7*, *Tlr8*, *Prps2*, *Msl3*, *Arphgap6*, and *Il1b* in bones, and that in BXSB-Yaa showed significant and negative correlations with S/B and *Il1a* and *Il1b* expression in bones. Tb.Wi showed significant and negative correlations with S/B, serum anti-dsDNA antibody levels, and the mRNA expression of *Rab9*, transcription elongation factor A (SII) N-terminal and central domain (*Tceanc*), *Tmsb4x*, *Tlr7*, *Tlr8*, *Prps2*, holocytochrome c synthase (*Hccs*), *Il1a*, and *Il1b* in bones, and that of BXSB-Yaa showed significant and negative correlations with oral-facial digital syndrome 1 (*Ofd1*), *Rab9*, *Tmsb4x*, *Il1a*, and *Il6* expression. The number of $TRAP^+$ osteoclasts showed significant and positive correlations with S/B, serum anti-dsDNA antibody levels, and mRNA expression of *Tlr8*, *Msl3*, *Arhgap6*, and *Mid1* in bones; and that in BXSB-Yaa showed significant and positive correlations with *Rab9* expression in bones. The numerical values of osteocalcin$^+$ osteoblast area showed significant and positive correlations with mRNA expression of *Amelx* in bones, and that in BXSB-Yaa showed significant and negative correlations with the *Tlr7* expression in bones.

Discussion

We clarified that the autoimmune disease-prone BXSB-Yaa had higher level of serum Ca at 2-4 months. Ca serum level is an indicator of bone metabolism, and hypercalcemia is predominantly caused by osteoclast activation as found in human osteoporosis with advancing age or menopause.[30,31] In fact, BXSB-Yaa showed an increase in the number of $TRAP^+$ osteoclasts from 3 months. Further, at 6 months, the serum level and urinary excretion of Ca in BXSB-Yaa significantly decreased and increased, respectively, with the progression of autoimmune disease phenotypes including nephritis. Although the renal tubules play a crucial role in the Ca reabsorption from primitive urine, the Ca could not be reabsorbed through renal tubules in aged BXSB-Yaa because of renal injury. Notably, secondary renal hyperparathyroidism was observed to develop to compensate the increased urinary loss of Ca in the CKD patients.[16] However, there was no change in the serum PTH level as well as the morphologies of thyroid and parathyroid glands in BXSB-Yaa during the examined periods. Importantly, in aged BXSB-Yaa, the tibia length and the weight of tibia and fibula were observed to significantly decrease compared with BXSB. Therefore, altered Ca dynamics in BXSB-Yaa suggested that their osteoclast number was increased and activated via a PTH-independent mechanism as a direct consequence of autoimmune disease or *Yaa* mutations to bone metabolism.

335 Previous studies have reported the development of hemolytic anemia, one of the causes of
336 osteoporosis, in mice carrying *Yaa* mutations.[32] Here, we also revealed that aged BXSB-Yaa
337 showed higher and lower values in MCV and MCHC, respectively compared to BXSB.
338 However, number of RBCs and Ht was comparable between both strains. A high value of
339 MCV signifies the production of large and immature RBCs including reticulocytes in
340 response to anemia.[33] MCHC indicated the hemoglobin concentration in RBC; generally, a
341 reduced MCHC was followed by a decrease in the MCV as found in microcytic hypochromic
342 anemia because of iron deficiency.[33] Alternatively, the altered patterns of MCV and MCHC in
343 BXSB-Yaa were not typical cases of anemia. Importantly, we also found significantly
344 increased numbers of WBCs and decreased PLs in aged BXSB-Yaa. Therefore, these data
345 reflect that the altered hematopoiesis, such as abnormal lymphocyte production as shown in
346 the previous study about human multiple myeloma,[34] might also affect the values of
347 hemoanalysis and BM morphology in BXSB-Yaa.
348
349 BXSB-Yaa tended to show an increase in osteoclasts and decrease in osteoblasts in the tibia at
350 3 months. These altered populations to bone resorption patterns would be associated with the
351 increased serum Ca level in BXSB-Yaa. Further, a sustained increase in osteoclast number
352 from 3 to 6 months would be critical for the abnormal remodeling of bones, as characterized
353 by significant reduction in bone length, weight, and trabeculas at 6 months. Importantly, the

354 osteocyte number was not altered, however, the bone area was reduced in the tibia of
355 BXSB-Yaa during periods of observation, indicating total decrease of osteocytes, important
356 cells for mineral metabolism.[35] Along with PTH, inflammatory cytokines including IL-1, IL-6,
357 and TNF-α can activate osteoclasts as found in the patients with RA and osteoporosis.[10–12]
358 However, these cytokines were not significantly correlated with the indices for bone
359 morphology and osteoclast numbers in the present study. Notably, in BXSB-Yaa, the
360 numerical values of osteoblasts was rescued at 6 months of age. However, the functional
361 maturation was not clear in the increased numerical values of osteoblasts in BXSB-Yaa. Thus,
362 the hyperimmune status in BM would be induced by autoimmune abnormality, and it might
363 indirectly affect the function and/or population of cells-associating bone remodeling in
364 BXSB-Yaa. Importantly, similar pathological alterations characterized by the loss of bone
365 tissue due to imbalance between osteoclasts and osteoblasts were observed in the osteoporosis
366 patients.[6] The patients of autoimmune disease also develop osteoporosis, for example, RA in
367 humans causes secondary osteoporosis due to inflammatory cytokines, medicine, or
368 immobilization.[36] Therefore, BXSB-Yaa would be a suitable model to analyze the altered
369 bone remodeling due to autoimmune abnormalities.
370
371 The causative factors of autoimmune disorder in BXSB-Yaa were encoded on the *Yaa* locus.[19]
372 We examined the expression of all 15 protein-coding genes on this locus to discuss their

373 pathological contributions of autoimmunity and bone morphology. At 3 months, *Rab9*,
374 *Tmsb4x*, *Prps2*, *Tlr7*, and *Tlr8* were highly expressed in BXSB-Yaa bones. There was no
375 relation between *Rab9* and autoimmunity. However, this gene was associated with osteoclast
376 function to secrete lysosomal enzymes in rats.[37] *Tmsb4x* is a diagnostic indicator of
377 osteoporosis or a regulator of the differentiation of hematopoietic cells in humans,[38,39] and
378 these genes were also significantly correlated with the indices of bone area in BXSB-Yaa.
379 *Prps2* also significantly correlated with the indices of bone area in BXSB-Yaa, and the
380 variants of *Prps2* genes were associated with the development of SLE in humans,[40] however,
381 there is no report on the bone. Furthermore, the associations of TLR7 or 8 and autoimmune
382 abnormalities were well analyzed in BXSB-Yaa,[22,41] and the roles of candidate genes in
383 developing SLE-like symptoms including nephritis were suggested. TLR7 was associated
384 with RA by contributing to produce inflammatory cytokines, such as IL-1, IL-6, and TNF-α,
385 from macrophages in mice.[42,43] TLR8 may have a role in human RA, however, the detailed
386 function of murine TLR8 is unclear.[44] Therefore, these genes would be candidates to develop
387 the autoimmune disease and/or following bone abnormalities.
388 The expression of *Msl3*, *Arhgap6*, *Amelx* and *Mid1* on *Yaa* locus significantly increased with
389 the progression of the autoimmune disease. However, there is no evidence between *Msl3* or
390 *Mid1* and autoimmunity or bones, but *Mid1* seemed to be associated with activating the innate
391 immune pathway in allergic asthma.[45] Alternatively, human *Arhgap6*, activating the Ras

homolog gene family, member A (RhoA),[46] and *Amelx* in mice seemed to act as the mediator of osteoblasts and osteoclasts-genesis, respectively.[47,48] Therefore, these genes would deteriorate autoimmune disease and/or bone abnormalities as exacerbating factors.

There were neither age nor strain-related differences in the expression of *Ofd1*, *Tceanc*, and *Hccs*. However, the expression of these genes had significant and negative correlation with Tb.Wi. Additionally, *Ofd1* seemed to be associated with endochondral skeletal development,[49] although there is no report of the evidence between *Tceanc* or *Hccs* and autoimmunity or bone study. Thus, these genes might also contribute to bone abnormality.

We have demonstrated that systemic autoimmune disease in BXSB-Yaa is closely associated with the morpho-functional abnormalities of bones including BM. The abnormalities are characterized by altered regulations of serum Ca, anemia tendency, and hematopoiesis with increased WBCs and decreased PLs, short length and low mass of long bones, imbalance in the populations of osteoclasts and osteoblasts, and increased expression of candidate genes for causing and/or exacerbating their phenotypes. Therefore, as shown in BXSB-Yaa, we concluded that the bone phenotypes in systemic autoimmune disease would elaborately be affected by the factors in the bone as well as the other immune and/or mineral metabolism organs.

Author contributions statement

T.N., O.I. and Y.K. designed and performed the experiments, and T.N., M.A.M., Y.O. S.O.K. and E.Y.H.A. provided the samples and analyzed the data. All authors were involved in writing the paper and have approved the final manuscript.

Declaration of conflicting interests

This manuscript has not been published or presented elsewhere in part or in entirety and is not under consideration by another journal. All authors have approved the manuscript and agree with submission to your esteemed journal. The authors declared no potential conflicts of interest with respect to the research, authorship, and/or publication of this article.

Funding statement

None.

References

1. Calvi LM, Adams GB, Weibrecht KW, Weber JM, Olson DP, Knight MC, Martin RP, Schipani E, Divieti P, Bringhurst FR, Milner LA, Kronenberg HM, Scadden DT. Osteoblastic cells regulate the haematopoietic stem cell niche. *Nature* 2003; **425**: 841–846.
2. Teitelbaum SL, Ross FP. Genetic regulation of osteoclast development and function. *Nat Rev Genet* 2003; **4**: 638–649.
3. Anderson DM, Maraskovsky E, Billingsley WL, Dougall WC, Tometsko ME, Roux ER, Teepe MC, DuBose RF, Cosman D, Galibert L. A homologue of the TNF receptor and its ligand enhance T-cell growth and dendritic-cell function. *Nature* 1997; **390**: 175–179.
4. Wong BR, Rho J, Arron J, Robinson E, Orlinick J, Chao M, Kalachikov S, Cayani E, Bartlett FS 3rd, Frankel WN, Lee SY, Choi Y. TRANCE is a novel ligand of the tumor necrosis factor receptor family that activates c-Jun N-terminal kinase in T cells. *J Biol Chem* 1997; **272**: 25190–25194.
5. Johnell O, Kanis JA. An estimate of the worldwide prevalence and disability associated with osteoporotic fractures. *Osteoporos Int* 2006; **17**: 1726–1733.
6. Rachner TD, Khosla S, Hofbauer LC. New horizons in osteoporosis. *Lancet Lond Engl* 2011; **377**: 1276–1287.
7. Villa A, Guerrini MM, Cassani B, Pangrazio A, Sobacchi C. Infantile malignant, autosomal recessive osteopetrosis: the rich and the poor. *Calcif Tissue Int* 2009; **84**: 1–12.
8. Firestein GS. Evolving concepts of rheumatoid arthritis. *Nature* 2003; **423**: 356–361.
9. Haugeberg G, Uhlig T, Falch JA, Halse JI, Kvien TK. Bone mineral density and frequency of osteoporosis in female patients with rheumatoid arthritis: Results from

394 patients in the Oslo County rheumatoid arthritis register. *Arthritis Rheum* 2000; **43**: 522-530.

10. Arend WP, Dayer J-M. Inhibition of the production and effects of interleukins-1 and tumor necrosis factor α in rheumatoid arthritis. *Arthritis Rheum* 1995; **38**: 151–160.

11. Iwakura Y. Roles of IL-1 in the development of rheumatoid arthritis: consideration from mouse models. *Cytokine Growth Factor Rev* 2002; **13**: 341–355.

12. Liu X-H, Kirschenbaum A, Yao S, Levine AC. Cross-Talk between the Interleukin-6 and Prostaglandin E_2 signaling systems results in enhancement of osteoclastogenesis through effects on the osteoprotegerin/receptor activator of nuclear factor-κB (RANK) ligand/RANK system. *Endocrinology* 2005; **146**: 1991–1998.

13. Rossini M, Viapiana O, Adami S, Idolazzi L, Fracassi E, Gatti D. Focal bone involvement in inflammatory arthritis: the role of IL17. *Rheumatol Int* 2016; **36**: 469–482.

14. Peacock M. Calcium metabolism in health and disease. *Clin J Am Soc Nephrol* 2010; **5 (Suppl 1)**: S23-30.

15. Pondel M. Calcitonin and calcitonin receptors: bone and beyond. *Int J Exp Pathol* 2000; **81**: 405–422.

16. Saliba W, El-Haddad B. Secondary hyperparathyroidism: pathophysiology and treatment. *J Am Board Fam Med* 2009; **22**: 574–581.

17. Agmon-Levin N, Theodor E, Segal RM, Shoenfeld Y. Vitamin D in systemic and organ-specific autoimmune diseases. *Clin Rev Allergy Immunol* 2013; **45**: 256–266.

18. Haywood MEK, Rogers NJ, Rose SJ, Boyle J, McDermott A, Rankin JM, Thiruudaian V, Lewis MR, Fossati-Jimack L, Izui S, Walport MJ, Morley BJ. Dissection of BXSB lupus phenotype using mice congenic for chromosome 1 demonstrates that separate intervals direct different aspects of disease. *J Immunol* 2004; **161**: 2753–2761.

19. Pisitkun P, Deane JA, Difilippantonio MJ, Tarasenko T, Satterthwaite AB, Bolland S.

476 Autoreactive B cell responses to RNA-related antigens due to TLR7 gene duplication.
477 *Science* 2006; **312**: 1669–1672.
478 20. Kawano S, Lin Q, Amano H, Kaneko T, Nishikawa K, Tsurui H, Tada N, Nishimura
479 H, Takai T, Shirai T, Takasaki Y, Hirose S. Phenotype conversion from rheumatoid
480 arthritis to systemic lupus erythematosus by introduction of *Yaa* mutation into
481 FcγRIIB-deficient C57BL/6 mice. *Eur J Immunol* 2013; **43**: 770–778.
482 21. Kimura J, Ichii O, Otsuka S, Sasaki H, Hashimoto Y, Kon Y. Close relations between
483 podocyte injuries and membranous proliferative glomerulonephritis in autoimmune
484 murine models. *Am J Nephrol* 2013; **38**: 27–38.
485 22. Kimura J, Ichii O, Miyazono K, Nakamura T, Horino T, Otsuka-Kanazawa S, Kon Y.
486 Overexpression of Toll-like receptor 8 correlates with the progression of podocyte
487 injury in murine autoimmune glomerulonephritis. *Sci Rep* 2014; **4**: 7290.
488 23. Kosenda K, Ichii O, Otsuka S, Hashimoto Y, Kon Y. BXSB/MpJ -*Yaa* mice develop
489 autoimmune dacryoadenitis with the appearance of inflammatory cell marker
490 messenger RNAs in the lacrimal fluid. *Clin Experiment Ophthalmol* 2013; **41**: 788–
491 797.
492 24. Schneider CA, Rasband WS, Eliceiri KW. NIH Image to ImageJ: 25 years of image
493 analysis. *Nat Methods* 2012; **9**: 671–675.
494 25. Parfitt AM, Drezner MK, Glorieux FH, Kanis JA, Malluche H, Meunier PJ, Ott SM,
495 Recker RR. Bone histomorphometry: Standardization of nomenclature, symbols, and
496 units: Report of the asbmr histomorphometry nomenclature committee. *J Bone Miner*
497 *Res* 1987; **2**: 595–610.
498 26. Chen S, Li J, Peng H, Zhou J, Fang H.Administration of erythropoietin exerts
499 protective effects against glucocorticoid-induced osteonecrosis of the femoral head in
500 rats. *Int J Mol Med* 2014; **33**: 840–848.
501 27. Minkin C. Bone acid phosphatase: Tartrate-resistant acid phosphatase as a marker of

502 osteoclast function. *Calcif Tissue Int* 1982; **34**: 285–290.
503 28. Ducy P, Zhang R, Geoffroy V, Ridall AL, Karsenty G. Osf2/Cbfa1: a transcriptional
504 activator of osteoblast differentiation. *Cell* 1997; **89**: 747–754.
505 29. Bendre MS, Montague DC, Peery T, Akel NS, Gaddy D, Suva LJ. Interleukin-8
506 stimulation of osteoclastogenesis and bone resorption is a mechanism for the increased
507 osteolysis of metastatic bone disease. *Bone* 2003; **33**: 28–37.
508 30. Jeremiah MP, Unwin BK, Greenawald MH. Diagnosis and management of
509 osteoporosis. *Am Fam Physician* 2015; **92(4)**: 261-268.
510 31. Riggs BL, Wahner HW, Seeman E, Offord KP, Dunn WL, Mazess RB, Johnson KA,
511 Melton LJ 3rd. Changes in bone mineral density of the proximal femur and spine with
512 aging. Differences between the postmenopausal and senile osteoporosis syndromes. *J*
513 *Clin Invest* 1982; **70**: 716–723.
514 32. Moll T, Martinez-Soria E, Santiago-Raber M-L, Amano H, Pihlgren-Bosch M,
515 Marinkovic D, Izui S. Differential activation of anti-erythrocyte and anti-DNA
516 autoreactive B lymphocytes by the Yaa mutation. *J Immunol* 2005; **174**: 702–709.
517 33. Moreno Chulilla JA, Romero Colás MS, Gutiérrez Martín M. Classification of anemia
518 for gastroenterologists. *World J Gastroenterol* 2009; **15**: 4627–4637.
519 34. Sharma S, Nemeth E, Chen Y-H, Goodnough J, Huston A, Roodman GD, Ganz T,
520 Lichtenstein A. Involvement of hepcidin in the anemia of multiple myeloma. *Clin*
521 *Cancer Res* 2008; **14**: 3262–3267.
522 35. Prideaux M, Findlay DM, Atkins GJ. Osteocytes: The master cells in bone
523 remodelling. *Curr Opin Pharmacol* 2016; **28**: 24–30.
524 36. McLendon AN, Woodis CB. A review of osteoporosis management in younger
525 premenopausal women. *Women's Heal* 2014; **10**: 59–77.
526 37. Zhao H, Ettala O, Väänänen HK. Intracellular membrane trafficking pathways in
527 bone-resorbing osteoclasts revealed by cloning and subcellular localization studies of

small GTP-binding rab proteins. *Biochem Biophys Res Commun* 2002; **293**: 1060–1065.

38. Borsy A, Podani J, Stéger V, Balla B, Horváth A, Kósa JP, Gyurján I Jr, Molnár A, Szabolcsi Z, Szabó L, Jakó E, Zomborszky Z, Nagy J, Semsey S, Vellai T, Lakatos P, Orosz L. Identifying novel genes involved in both deer physiological and human pathological osteoporosis. *Mol Genet Genomics* 2009; **281**: 301–313.

39. Shimamura R, Kudo J, Kondo H, Dohmen K, Gondo H, Okamura S, Ishibashi H, Niho Y. Expression of the thymosin beta 4 gene during differentiation of hematopoietic cells. *Blood* 1990; **76**: 977-984.

40. Zhang Y, Zhang J, Yang J, Wang Y, Zhang L, Zuo X, Sun L, Pan HF, Hirankarn N, Wang T, Chen R, Ying D, Zeng S, Shen JJ, Lee TL, Lau CS, Chan TM, Leung AM, Mok CC, Wong SN, Lee KW, Ho MH, Lee PP, Chung BH, Chong CY, Wong RW, Mok MY, Wong WH, Tong KL, Tse NK, Li XP, Avihingsanon Y, Rianthavorn P, Deekajorndej T, Suphapeetiporn K, Shotelersuk V, Ying SK, Fung SK, Lai WM, Wong CM, Ng IO, Garcia-Barcelo MM, Cherny SS, Tam PK, Sham PC, Yang S, Ye DQ, Cui Y, Zhang XJ, Lau YL, Yang W. Meta-analysis of GWAS on two Chinese populations followed by replication identifies novel genetic variants on the X chromosome associated with systemic lupus erythematosus. *Hum Mol Genet* 2015; **24**: 274–284.

41. Santiago-Raber M-L, Kikuchi S, Borel P, Uematsu S, Akira S, Kotzin BL, Izui S. Evidence for genes in addition to Tlr7 in the Yaa translocation linked with acceleration of systemic lupus erythematosus. *J Immunol* 2008; **181**: 1556–1562.

42. Alzabin S, Kong P, Medghalchi M, Palfreeman A, Williams R, Sacre S. Investigation of the role of endosomal Toll-like receptors in murine collagen-induced arthritis reveals a potential role for TLR7 in disease maintenance. *Arthritis Res Ther* 2012; **14**: R142.

554 43. Huang Q-Q, Pope RM. The role of toll-like receptors in rheumatoid arthritis. *Curr*
555 *Rheumatol Rep* 2009; **11**: 357–364.
556 44. Sacre SM, Lo A, Gregory B, Simmonds RE, Williams L, Feldmann M, Brennan FM,
557 Foxwell BM. Inhibitors of TLR8 reduce TNF production from human rheumatoid
558 synovial membrane cultures. *J Immunol* 2008; **181**: 8002–8009.
559 45. Collison A, Hatchwell L, Verrills N, Wark PA, de Siqueira AP, Tooze M, Carpenter H,
560 Don AS, Morris JC, Zimmermann N, Bartlett NW, Rothenberg ME, Johnston SL,
561 Foster PS, Mattes J. The E3 ubiquitin ligase midline 1 promotes allergen and
562 rhinovirus-induced asthma by inhibiting protein phosphatase 2A activity. *Nat Med*
563 2013; **19**: 232–237.
564 46. Prakash SK, Paylor R, Jenna S, Lamarche-Vane N, Armstrong DL, Xu B, Mancini
565 MA, Zoghbi HY. Functional analysis of ARHGAP6, a novel GTPase-activating
566 protein for RhoA. *Hum Mol Genet* 2000; **9**: 477–488.
567 47. McBeath R, Pirone DM, Nelson CM, Bhadriraju K, Chen CS. Cell Shape, cytoskeletal
568 tension, and RhoA regulate stem cell lineage commitment. *Dev Cell* 2004; **6**: 483–495.
569 48. Jacques J, Hotton D, De la Dure-Molla M, Petit S, Asselin A, Kulkarni AB, Gibson
570 CW, Brookes SJ, Berdal A, Isaac J. Tracking endogenous amelogenin and
571 ameloblastin in vivo. *PLoS One* 2014; **9**: e99626.
572 49. Bimonte S, De Angelis A, Quagliata L, Giusti F, Tammaro R, Dallai R, Ascenzi MG,
573 Diez-Roux G, Franco B. Ofd1 is required in limb bud patterning and endochondral
574 bone development. *Dev Biol* 2011; **349**: 179–191.
575

Figure legends

Figure 1. Autoimmune disease-associated phenotypes, serological and hematological analysis, and urinalysis in mice. (a)Body weight (BW). (b) The ratio of spleen weight to BW (S/B). (c) The serum levels of anti-double strand DNA (dsDNA) antibody. (d) Serum calcium (Ca) level. (e) The ratio of urinary Ca to creatinine (CRE) level. (f) Serum parathyroid hormone (PTH) level. (g) The number of white blood cells (WBCs). (h) The number of red blood cells (RBCs). (i) The number of platelets (PLs). (j) Hematocrit concentration (HC). (k) Hematocrit volume (Ht). (l) Mean corpuscular volume (MCV). (m) Mean corpuscular HC (MCHC). (n) Blood smear. Some reticulocytes (arrows) are observed in the smear of BXSB-Yaa at 6 months. Diff-Quik staining. Bars = 50 μm. BXSB: BXSB/MpJ. BXSB-Yaa: BXSB/MpJ-*Yaa*. The numbers of samples used in the studies are as follows: n = 8-18 (a and b), n = 5-10 (c), n = 9-16 (d), n = 5 (e), n = 8-18 (f), and n = 4-9 (g-m). Each bar represents the mean ± SE. *: Significance with the other strain at the same age (Mann-Whitney *U*-test, $*P < 0.05$, $**P < 0.01$). †: Significance with the same strain at other age (Mann-Whitney *U*-test, $\dagger P < 0.05$, $\dagger\dagger P < 0.01$).

Figure 2. Histology of thyroid and parathyroid glands in mice. (a) Renal histology. Severe glomerulonephritis (asterisks) and cell infiltrations into the tubulointerstitium (arrow) are observed in the kidneys of BXSB-Yaa at 6 months. PAS staining. (b) Thyroid glands. Immunohistochemistry for calcitonin. Neither age nor strain- related changes are observed in the organ. (c) Parathyroid glands. Immunohistochemistry for parathyroid hormone. Neither age nor strain-related changes are observed in each organ. BXSB: BXSB/MpJ. BXSB-Yaa: BXSB/MpJ-*Yaa*. The number of samples used in the studies is as follows: n = 4 (a), n = 5-12 (b), and n = 4-8 (c). Bars = 100 μm.

Figure 3. Morphological differences of bones in mice. (a) Gross morphology of bones. At 6

602 months, the tibia and fibula of BXSB/MpJ-*Yaa* (BXSB-*Yaa*) is macroscopically smaller, and
603 its bone marrow (BM) is whiter compared with BXSB/MpJ (BXSB). Bars = 10 mm. (b) Tibia
604 length. (c) Tibia and fibula weight. (d) The ratio of tibia and fibula weight to body weight
605 (BW). (e) Tibia histology. The reduction of trabeculas and thinning of compact bone are
606 observed in BXSB-Yaa at 6 months. Neither age nor strain-related differences in the number
607 of osteocytes (arrows) are observed. HE staining. Bars = 100 μm. (f) The area ratio of bone to
608 bone marrow (BM). (g) The ratio of trabecular area to tissue area (Tb.Ar/T.Ar). (h) Trabecular
609 width (Tb.Wi). (i) Trabecular number (Tb.N). (j) Trabecular separation (Tb.Sp). (k) The
610 density of osteocytes. BXSB: BXSB/MpJ. BXSB-Yaa: BXSB/MpJ-*Yaa*. The number of
611 samples used in the studies is as follows: n = 4-14. Each bar represents the mean ± SE. *:
612 significance with the other strain at same age (Mann-Whitney *U*-test, *$P < 0.05$, **$P < 0.01$).
613 †: significance with the same strain at other age (Mann-Whitney *U*-test, †$P < 0.05$, ††$P <$
614 0.01).
615
616 **Figure 4. Altered number of osteoclasts and osteoblasts in mouse bones.** (a) Tibia
617 histology stained by tartrate-resistant acid phosphatase (TRAP) for osteoclast detection.
618 $TRAP^+$ osteoclasts (arrows) in all mice are mainly localized to the surface of the medullary
619 cavity, especially near the epiphyseal cartilages, and seem to elicit a stronger reaction in
620 BXSB-Yaa at 6 months compared with the other mice. (b) Tibia histology stained by
621 immunohistochemistry of osteocalcin for osteoblasts. The numerical values of $osteocalcin^+$
622 osteoblasts (arrow heads), also localized to surface of medullary, seems to be lesser in
623 BXSB-Yaa compared with BXSB at 3 months. (c) The number of positive cells for TRAP. (d)
624 The numerical values of positive cells for osteocalcin. BXSB: BXSB/MpJ. BXSB-Yaa:
625 BXSB/MpJ-*Yaa*. Bars = 100 μm. The number of samples used in the studies is as follows: n =
626 5-12. Each bar represents the mean ± SE. *: significance with the other strain at the same age
627 (Mann-Whitney *U*-test, $P < 0.05$).

Figure 5. mRNA expression of *Yaa* locus genes and inflammatory cytokines in the bones of mice. The genes on *Yaa* locus, such as *Rab9*, *Tmsb4x*, *Tlr8*, *Tlr7*, and *Prps2*, are higher in BXSB-Yaa compared with BXSB at both ages. Additionally, BXSB-Yaa at 6 months also significantly shows higher expression in *Msl3* and *Arhgap6* compared with BXSB and BXSB-Yaa at 3 months, respectively. Age-related significant increase is observed in the expression of *Amelx* in BXSB-Yaa, and this strain at 6 months also significantly shows higher expression in *Mid1* than BXSB. The mRNA levels of inflammatory cytokines, such as *Il1a* and *Tnf*, in BXSB-Yaa at 6 months are significantly higher than in BXSB at the same age and in BXSB-Yaa at 3 months. Further, an age-related significant increase is observed in the mRNA levels of *Il1b* in both strains. BXSB: BXSB/MpJ. BXSB-Yaa: BXSB/MpJ-*Yaa*. The number of samples used in the studies is as follows: n = 5-15. Each bar represents the mean ± SE. *: significance with the other strain at the same age (Mann-Whitney *U*-test, $*P < 0.05$, $**P < 0.01$). †: significance with the same strain at other ages (Mann-Whitney *U*-test, $\dagger P < 0.05$, $\dagger\dagger P < 0.01$).

Figure 1

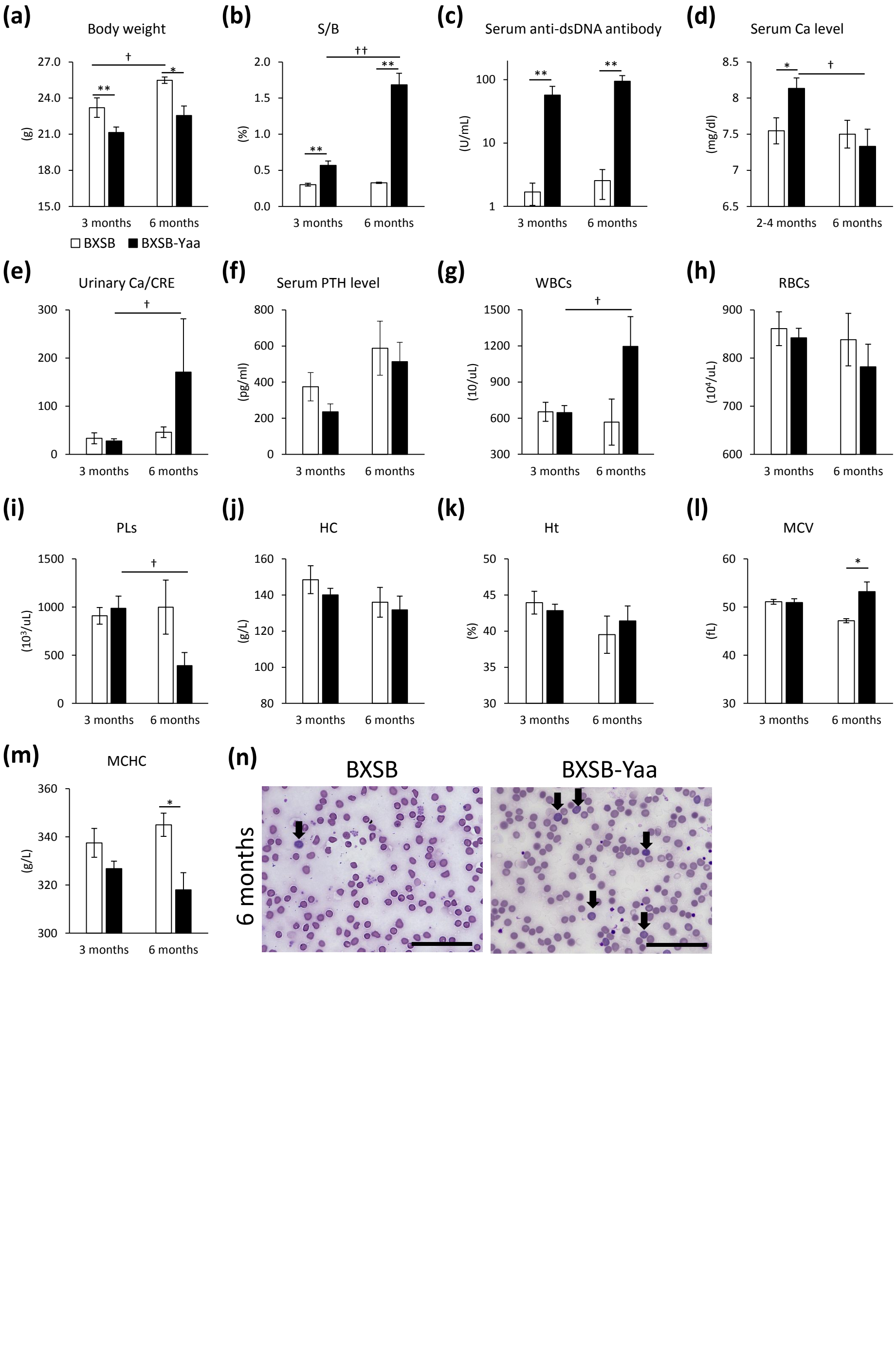
(a)
Body weight
(g)
27.0
24.0
21.0
18.0
15.0
†
**
*
3 months
6 months
□ BXSB ■ BXSB-Yaa
(b)
S/B
(%)
2.0
1.5
1.0
0.5
0.0
††
**
**
3 months
6 months
(c)
Serum anti-dsDNA antibody
(U/mL)
100
10
1
**
**
3 months
6 months
(d)
Serum Ca level
(mg/dl)
8.5
8
7.5
7
6.5
*
†
2-4 months
6 months
(e)
Urinary Ca/CRE
300
200
100
0
†
3 months
6 months
(f)
Serum PTH level
(pg/ml)
800
600
400
200
0
3 months
6 months
(g)
WBCs
(10/uL)
1500
1200
900
600
300
†
3 months
6 months
(h)
RBCs
(10⁴/uL)
900
800
700
600
3 months
6 months
(i)
PLs
(10³/uL)
1500
1000
500
0
†
3 months
6 months
(j)
HC
(g/L)
160
140
120
100
80
3 months
6 months
(k)
Ht
(%)
50
45
40
35
30
3 months
6 months
(l)
MCV
(fL)
60
50
40
30
*
3 months
6 months
(m)
MCHC
(g/L)
360
340
320
300
*
3 months
6 months
(n)
BXSB
BXSB-Yaa
6 months

Figure 2

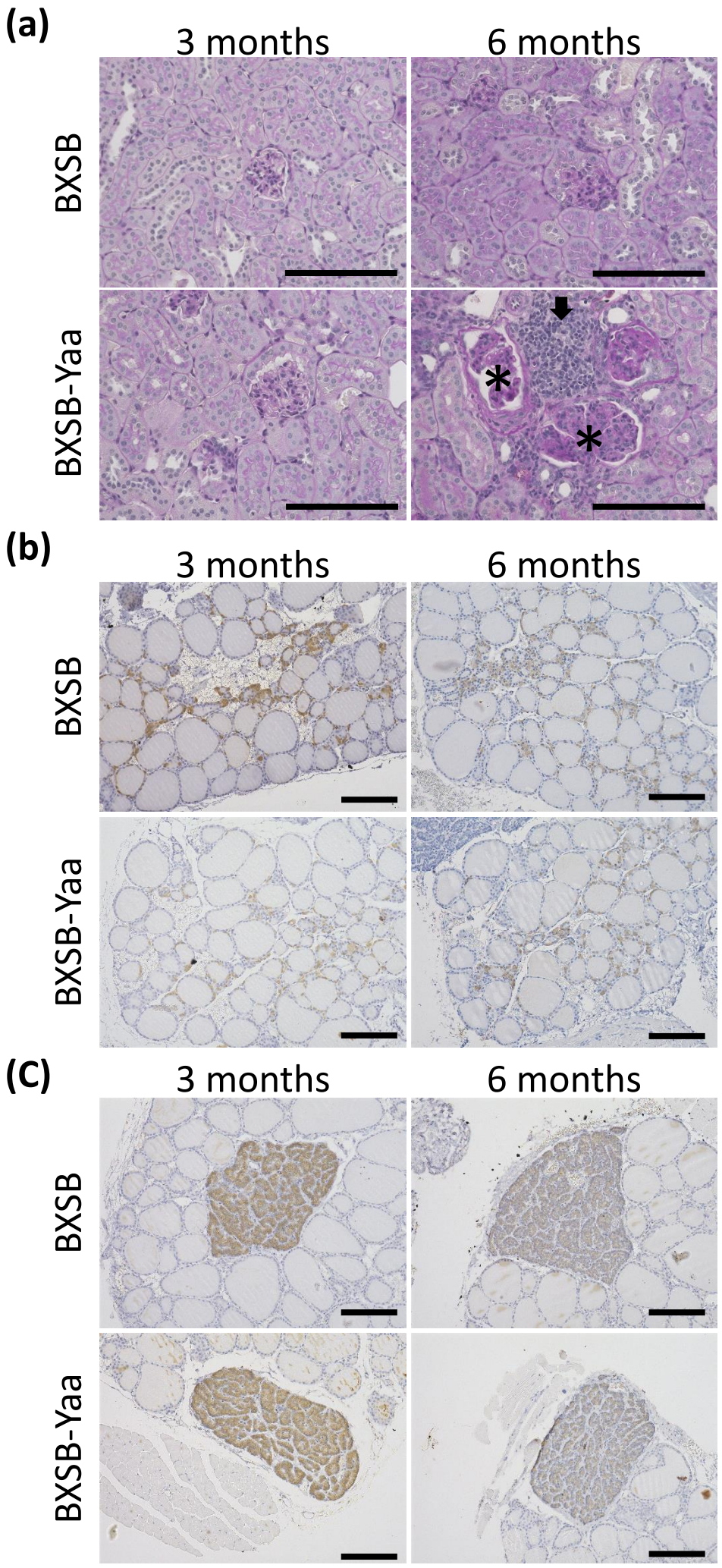
(a)
3 months
6 months
BXSB
BXSB-Yaa
(b)
3 months
6 months
BXSB
BXSB-Yaa
(C)
3 months
6 months
BXSB
BXSB-Yaa

Figure 3

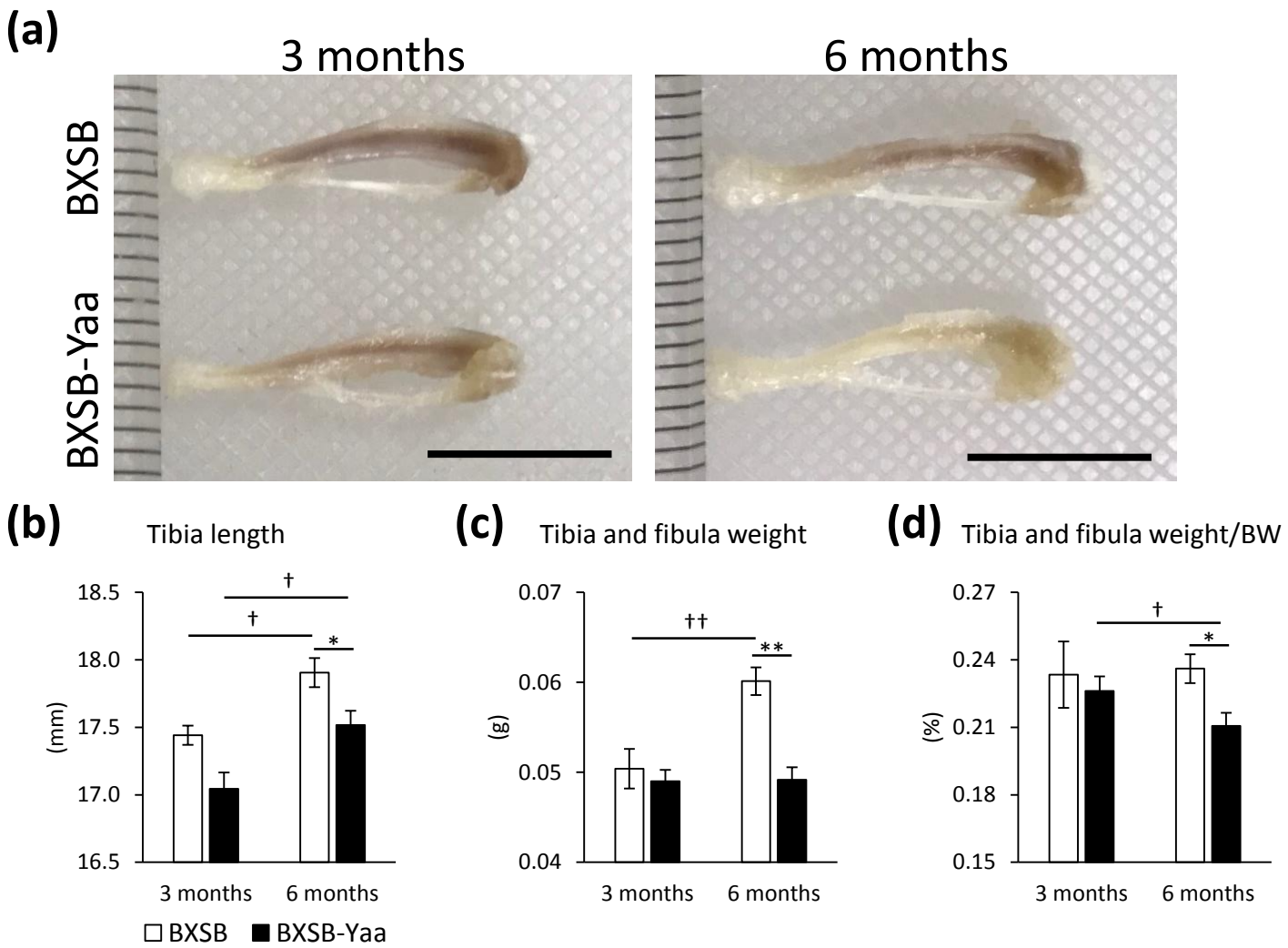
(a)
3 months
6 months
BXSB
BXSB-Yaa
(b)
Tibia length
(mm)
18.5
18.0
17.5
17.0
16.5
†
†
*
3 months
6 months
BXSB
BXSB-Yaa
(c)
Tibia and fibula weight
(g)
0.07
0.06
0.05
0.04
††
**
3 months
6 months
(d)
Tibia and fibula weight/BW
(%)
0.27
0.24
0.21
0.18
0.15
†
*
3 months
6 months
(e)
3 months
6 months
BXSB
BXSB-Yaa
(f)
Area ratio of bone to BM
1.2
1.0
0.8
0.6
0.4
*
3 months
6 months
(g)
Tb.Ar/T.Ar
(%)
0.3
0.2
0.1
0.0
†
**
3 months
6 months
(h)
Tb.Wi
(μm)
50.0
40.0
30.0
20.0
†
**
**
3 months
6 months
(i)
Tb.N
(mm-1)
6.0
4.5
3.0
1.5
0.0
†
**
3 months
6 months
(j)
Tb.Sp
(μm)
2400
1800
1200
600
0
†
**
3 months
6 months
(k)
Density of osteocytes
(Number/mm2)
800
600
400
200
0
3 months
6 months

Figure 4

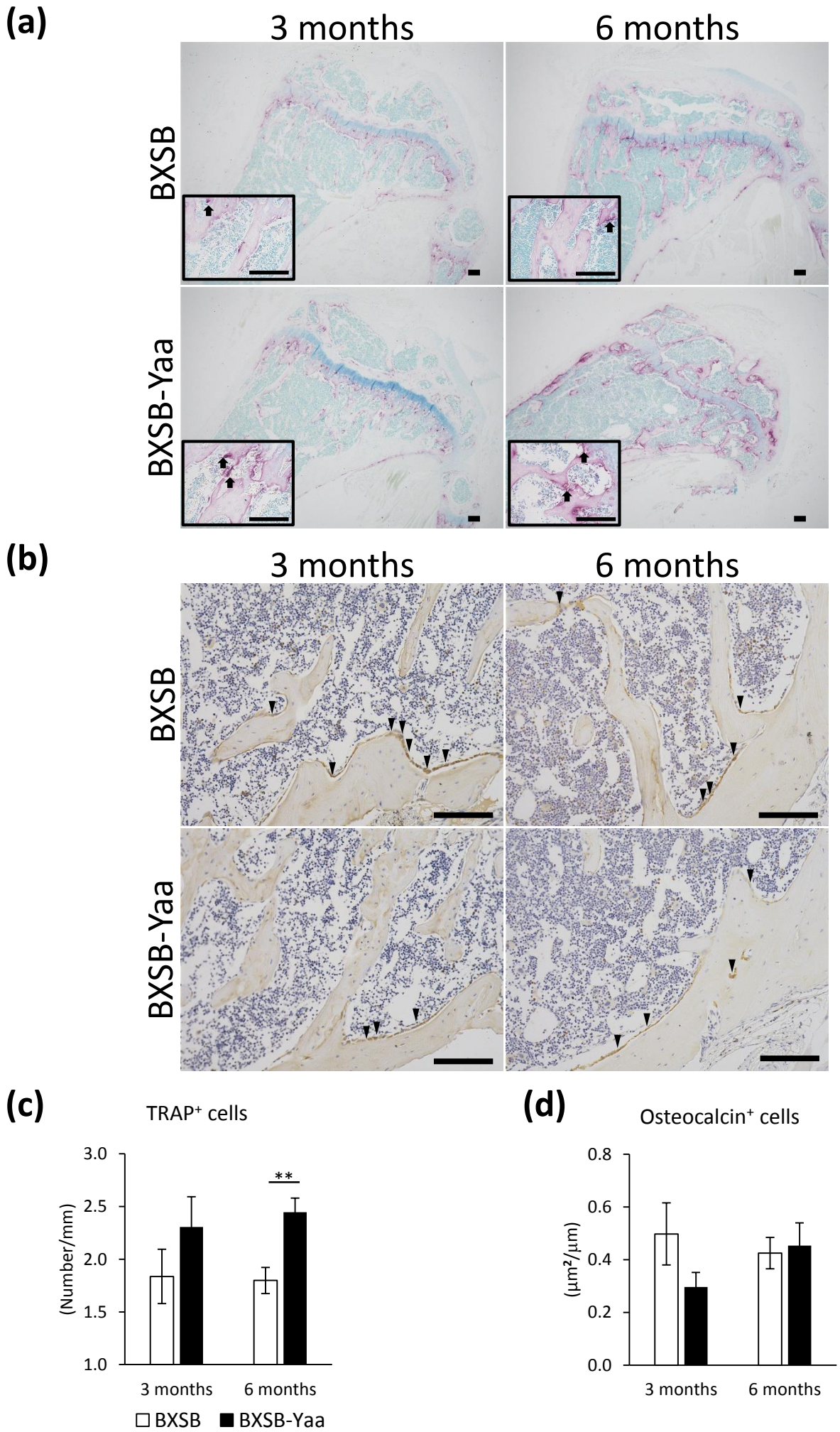
(a)
3 months
6 months
BXSB
BXSB-Yaa
(b)
3 months
6 months
BXSB
BXSB-Yaa
(c)
TRAP+ cells
(Number/mm)
3.0
2.5
2.0
1.5
1.0
**
3 months
6 months
BXSB
BXSB-Yaa
(d)
Osteocalcin+ cells
(μm²/μm)
0.8
0.6
0.4
0.2
0.0
3 months
6 months

Figure 5

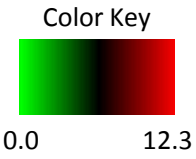

		3 months		6 months	
		BXSB	BXSB-Yaa	BXSB	BXSB-Yaa
Gene on *Yaa* locus	*Ofd1*	1.0	0.8	0.7	0.8
	Trppc2	0.0	0.0	0.0	0.0
	Rab9	1.0	1.7 **	0.8	1.9 **
	Tceanc	1.0	1.3	0.6	1.0
	Egfl6	1.3	0.5	0.7	0.3
	Tmsb4x	1.0	2.0 *	1.0	2.9 **
	Tlr8	1.0	1.8 *	0.8	3.2 **
	Tlr7	1.0	3.0 **	0.9	4.0 **
	Prps2	1.1	2.0 **	1.3	2.6 **
	Frmpd4	1.4	2.2	1.8	5.4
	Msl3	2.0	3.1	2.2	12.3 ** ††
	Arhgap6	1.0	1.3	0.8	3.0 ** ††
	Amelx	1.4	1.7	4.1	3.6 †
	Hccs	1.0	1.8	1.1	2.0
	Mid1	1.0	1.2	0.8	1.7 *
Inflammatory cytokine	*Il1a*	1.0	0.9	0.8	1.7 ** ††
	Il1b	1.1	1.1	2.6 †	3.9 ††
	Il6	1.0	0.7	1.5	1.1
	Il8	1.0	0.8	0.6	0.4
	Tnf	1.1	0.6	0.8	1.4 * †

Table 1. Correlations between bone morphological parameters and autoimmune disease indices or gene expression.

	Strains	Parameters					
		TF/B	Bone area	Tb.Ar/T.Ar	Tb.Wi	Osteoclast	Osteoblast
S/B	All mice	-0.407*	0.117	-0.660**	-0.665**	0.470**	-0.01
	BXSB-Yaa	-0.144	0.401	-0.476*	-0.399	0.161	0.074
Anti-dsDNA antibody	All mice	-0.331	-0.523*	-0.621**	-0.452*	0.702**	0.079
	BXSB-Yaa	-0.233	0.048	0.033	0.300	0.583	0.314
Ofd1	All mice	0.321	-0.296	-0.049	0.092	-0.218	-0.01
	BXSB-Yaa	0.771	-0.214	-0.095	-0.738*	-0.619	-0.214
Rab9	All mice	-0.100	-0.591**	-0.259	-0.680**	0.094	0.022
	BXSB-Yaa	0.600	-0.310	-0.095	-0.762*	-0.738*	-0.071
Tceanc	All mice	-0.132	-0.286	-0.236	-0.534*	0.230	-0.179
	BXSB-Yaa	0.029	0.071	-0.286	-0.238	0.238	-0.036
Egfl6	All mice	-0.312	0.263	0.032	0.238	0.082	0.091
	BXSB-Yaa	-0.257	0.476	0.048	0.500	0.381	-0.357
Tmsb4x	All mice	-0.056	-0.575*	-0.397*	-0.684**	0.288	-0.221
	BXSB-Yaa	0.371	-0.738*	-0.524	-0.881**	-0.619	0.250
Tlr8	All mice	-0.449*	-0.050	-0.574**	-0.618**	0.539**	0.054
	BXSB-Yaa	-0.181	0.091	-0.389	-0.221	0.276	0.005
Tlr7	All mice	-0.399*	0.175	-0.397*	-0.684**	0.288	-0.221
	BXSB-Yaa	0.011	0.456	-0.221	-0.482	0.009	-0.670*
Prps2	All mice	-0.282	-0.558*	-0.585*	-0.686**	0.399	0.216
	BXSB-Yaa	0.429	-0.738*	-0.5	-0.524	-0.095	0.286
Frmpd4	All mice	-0.240	-0.432	-0.318	0.071	0.393	0.231
	BXSB-Yaa	-0.486	-0.607	-0.214	0.000	0.143	0.486
Msl3	All mice	-0.188	-0.639**	-0.544*	-0.364	0.488*	0.223
	BXSB-Yaa	-0.600	-0.929**	-0.667	-0.429	0.024	0.357
Arhgap6	All mice	-0.418	-0.577*	-0.505*	-0.377	0.680**	0.093
	BXSB-Yaa	-0.886*	-0.595	-0.357	0.143	0.619	0.750
Amelx	All mice	-0.086	-0.047	-0.038	0.350	0.224	0.600*
	BXSB-Yaa	-0.657	-0.69	-0.476	0.048	0.452	0.571
Hccs	All mice	0.018	-0.444	-0.36	-0.495*	0.159	0.132

	BXSB-Yaa	0.200	-0.357	-0.143	-0.548	-0.381	-0.071
Mid1	All mice	-0.276	-0.585*	-0.255	-0.327	0.486*	0.152
	BXSB-Yaa	-0.657	-0.333	-0.167	0.071	0.500	0.714
Il1a	All mice	-0.252	0.212	-0.326	-0.444*	0.010	0.154
	BXSB-Yaa	-0.133	0.362	-0.550*	-0.536*	-0.124	0.143
Il1b	All mice	-0.306	0.225	-0.579**	-0.440*	0.111	0.072
	BXSB-Yaa	-0.125	0.159	-0.554*	-0.468	-0.041	0.214
Il6	All mice	0.385	0.265	0.051	0.036	-0.294	0.100
	BXSB-Yaa	-0.200	-0.429	-0.619	-0.714*	-0.214	-0.100
Il8	All mice	0.046	-0.017	0.235	0.078	-0.142	-0.236
	BXSB-Yaa	0.700	0.25	0.143	-0.643	-0.357	-0.600
Tnf	All mice	-0.050	-0.066	0.026	0.037	0.047	0.056
	BXSB-Yaa	-0.432	-0.095	-0.218	-0.024	0.037	0.136

Spearman's lank correlation coefficients. *: $P < 0.05$, **: $P < 0.01$, $n \geq 4$. BXSB-Yaa: BXSB/MpJ-Yaa, S/B: Ratio of spleen weight to body weight, TF/B: Ratio of tibia and fibula weight to body weight, Bone area: Area ratio of bone to bone marrow, Tb.Ar/T.Ar: The ratio of bone area to tissue area, Tb.Wi: Trabecular width, Tb.N: Trabecular number, Tb.Sp: Trabecular separation, Osteoclasts: Number of TRAP+ osteoclasts, Osteoblasts: Numerical values of osteocalcin+ osteoblasts.